

Advance Publication Cover Page



**Cooperative Effect of Spacer and Lewis Base on Highly Reversible Spectral
Changes of the Octaethylporphyrin Chromatic System in Sensitivity,
Stability, and Visibility to Trifluoroacetic Acid**

Hideto Kempe, Junya Yamamoto, Miki Ishida, Nobutomo Takahashi, Junro Yoshino, Naoto Hayashi,
and Hiroyuki Higuchi*

Advance Publication on the web July 15, 2016 by J-STAGE

doi:10.1246/bcsj.20160176

© 2016 The Chemical Society of Japan

Cooperative Effect of Spacer and Lewis Base on Highly Reversible Spectral Changes of The Octaethylporphyrin Chromatic System in Sensitivity, Stability, and Visibility to Trifluoroacetic Acid

Hideto KEMPE,¹ Junya YAMAMOTO,² Miki ISHIDA,² Nobutomo TAKAHASHI,² Junro YOSHINO,² Naoto HAYASHI,² and Hiroyuki HIGUCHI^{1,2*}

¹Graduate School of Innovative Life Science, University of Toyama,

²Graduate School of Science and Engineering, University of Toyama,

3190 Gofuku, Toyama, Toyama 930-8555, Japan

*E-mail address: higuchi@sci.u-toyama.ac.jp (H. Higuchi)

Abstract

The diacetylene-group connected chromatic system of [octaethylporphyrin]-[spacer]-[Lewis base] triads (OEP-SPC-LB) was conclusively studied, in which a trigger-like interaction of the terminal LB with trifluoroacetic acid (TFA) dramatically affects the inherent electronic properties of OEP. The ¹H NMR, IR, and electronic absorption spectral properties of these OEP derivatives were examined, and were contemplated in view of a cooperative effect of SPC and LB on their OEP nucleus. Based on the results from this study, the structural elements for molecular design will be proposed in order to improve their reversible spectral changes between neutral and acidic media in terms of sensitivity, stability, and visibility to TFA.

1. Introduction

Porphyrin nucleus is a natural pigment of particularly great interests in not only photo-sensitized reactions¹ but also in redox respiratory system,² duly to possess its high sensitivity to the trigger-like stimuli such as light and oxygen, swiftly to transform itself to a meta-stable state in response to those stimuli, and readily to recover its original state by release from those outside stimuli. In those sequential reversible processes between these transitory states, chemically oxidative-reductive reactions are smoothly performed in the living bodies regularly and repeatedly. Modeling on such a sustainable mechanism taken in the natural world, in recent years, the artificially functional porphyrin-based materials of various types sensitive to pH,³ metal-ions,⁴ temperature,⁵ light,^{1,6} and so forth, have been vastly demonstrated, by connecting those electronic and structural properties with particular spectral changes at each state. In relation with such drastic development of organic functional materials science, we have been also engaged in the study of various unique octaethylporphyrin (OEP) derivatives, aiming at the highly performable system especially sensing to organic acids and/or to electrochemical operations.⁷

Our original OEP chromatic system in the present study carries Lewis base (LB) at one terminal position in the π -electronic conjugation chain and dihexyl-2,2'-bithiophene (DHBTh) as a spacer (SPC) in its middle position (**Chart 1**), described as OEP-DHBTh-LB, in which all the three components are combined with a skeletally rigid but π -electronically mobile linkage of 1,3-butadiyne (diacetylene) (**Chart 2**).⁸ A whole molecular planarity in its π -electronic conjugation system is readily adjusted by an orientation of the two 3-hexylthiophene (3HTH) rings in DHBTh; head-to-head (HH) or head-to-tail (HT) or tail-to-tail (TT).⁹ Yet, since the

three OEP, DHBTh, and LB components are connected with the diacetylene linkage, the skeletal features such as conformation and geometry are almost the same in each DHBTh set of derivatives, regardless of LB, due to no steric hindrance between them (wide infra). Therefore, the OEP-DHBTh-LB system would be placed in a well-defined structural system, suitable for analysis and evaluation of the effect from each component DHBTh or LB on the spectrum-property relationships of these OEP derivatives between neutral and acidic conditions.

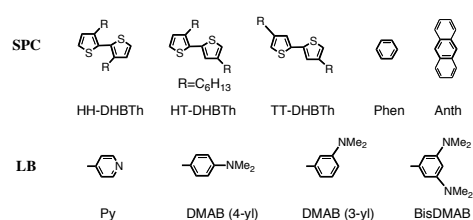


Chart 1. Abbreviation of SPC and LB in OEP-SPC-LB.

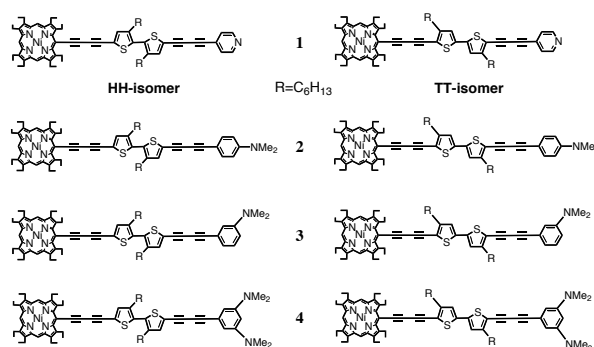


Chart 2. An extended π -electronic conjugation system of OEP-DHBTh-LB (1-4).

So far, it has been revealed in this system that addition of trifluoroacetic acid (TFA: pK_a 0.23)¹⁰ into its sample solution changes both ¹H NMR and electronic absorption spectra via the two-steps processes. The first step process corresponds to the regular changes arising from a simple protonation of TFA on the N atom of LB, and the second step process corresponds to the drastic changes arising from a direct interaction of TFA onto the OEP component (**Chart 3**, vide infra).¹¹ Yet, it has been experimentally demonstrated that quenching TFA with ordinary bases like triethylamine (NEt₃) recovers their original spectra quite well. This is a common phenomenon of OEP-DHBTh-LB in the reversible spectral changes, as well as the solution-color changes, with DHBTh and LB reflecting on the electronic structure of OEP.

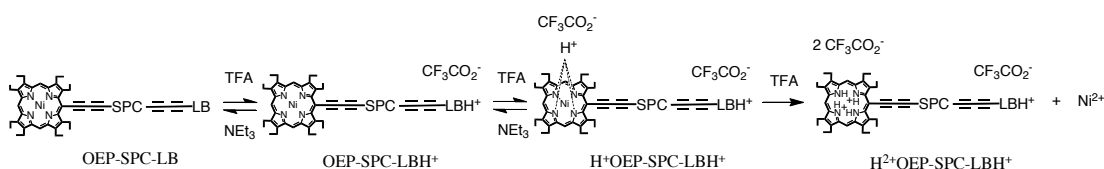


Chart 3. The protonation processes of OEP-SPC-LB with TFA at the first and second stages.

Based on the TFA-sensing examinations (*vide infra*), it has been proved that the sensitivity to TFA of this system increases in order of $2 << 3 < 1$ and its reversible stability increases in order of $1 << 2 < 3$, suggesting that the derivative **3** is rather promising in both sensitivity and stability.¹¹ These results indicate that the lone-pair electrons on the N atom of LB stereo-electronically plays an important role in an extended π -electronic conjugation chain of this system prior to the proton-acceptable ability (basicity) of LB, since the conjugated acids of pyridine (Py) and *N,N*-dimethylaminobenzene (DMAB) themselves are well known to possess almost the same pK_a value as each other (5.14 for Py- H^+ and 5.06 for DMAB- H^+) (**Chart 4**).¹⁰ Accordingly, taking this consequence into consideration, 3,5-bis(*N,N*-dimethylamino)benzene (BisDMAB: $pK_{a(1)}$ 2.65 and $pK_{a(2)}$ 4.88)¹² could be a promising LB for enhancing their sensitivity and stability to TFA (**Chart 1**). As expected, among **1-4**, the derivative **4** showed the highest function in both sensitivity and stability (**Chart 2**).¹¹

In addition to these two valuations (sensitivity and stability), another essential one for the acid-sensing materials is to put the visibility, *i.e.*, to construct the molecular structure with the greater spectral changes in magnitude between neutral and acidic conditions.³⁻⁶ The higher visibility means the more performable functions in accuracy, leading to the more sophisticated material. And, our aim and goal in this research is to achieve a methodology for producing the desired electronic structures of OEP purposively, without changing their skeletal features, by choosing an adequate pair of SPC and LB like a building-brick from a wide variety of SPC and LB. Previously it was shown from the electronic spectral study with **1-4** that the TT-DHBTh SPC with the higher π -electronic conjugation plane brings the greater spectral changes into their Soret- and Q-bands,^{13, 14} than the HH isomer.¹¹ Moreover, from the consequence performed with the diacetylene-group connected dimeric OEP derivatives (OEP-SPC-OEP), it was suggested that an introduction of SPC with the higher mobile π -electrons is preferable to an extension of π -electronic conjugation into the skeletal chain, for further enhancement of their visibility.¹⁵

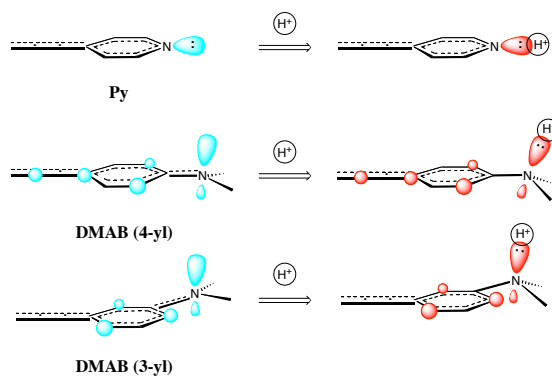


Chart 4. Delocalization mode of the lone pair electrons (\circ) on the N atom of LB (left). Distribution mode of the positive charge (\circ) of the N-protonated species LBH⁺ (right).

In our continuous investigations of OEP-SPC-LB toward the higher functionality in respect of those three valuations (sensitivity, stability, and visibility), the OEP-SPC-LB derivatives **5-10** were newly synthesized. In this study, benzene (abbreviated as Phen) and anthracene (Anth) are employed as SPC, while Py, DMAB, and BisDMAB are employed as LB (**Charts 1** and **5**). The structure-property relationships of **5-10** were conclusively studied, as compared with those of the DHBTh derivatives **1-4**. Basically, the behaviors of OEP-SPC-LB between before and after the protonation processes were examined by means of ¹H NMR and electronic absorption spectral measurements, and were comparatively analyzed in terms of the inductive and conjugation effects on their spectral changes. Successively, their relative sensitivity and reversible stability to TFA were estimated, on the basis of the minimum amount of TFA necessary for completion of the spectral changes at each stage. Then, toward our final goal, the structurally tractable elements in the present OEP chromatic system will be proposed, in order to derive a guideline for further enhancement of the proton-sensing functionality in sensitivity, stability, and visibility.

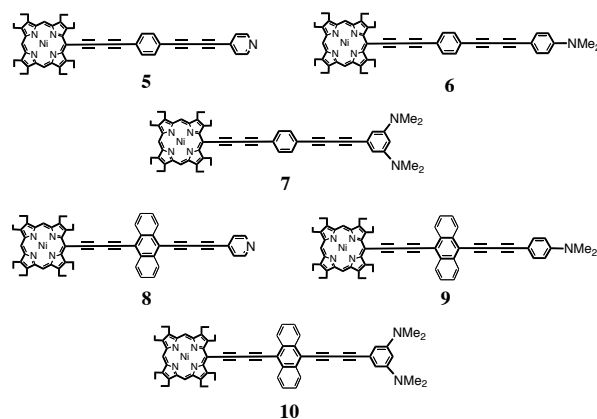


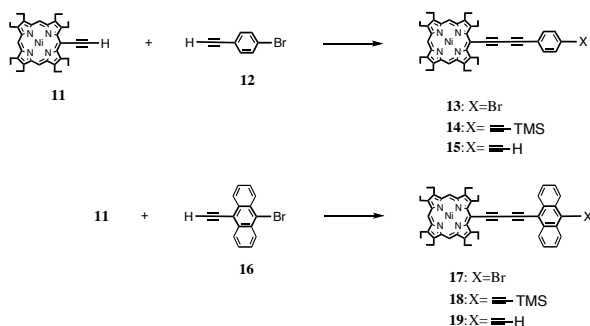
Chart 5. Diacetylene-group connected OEP-SPC-LB derivatives **5-10**.

2. Results and Discussion

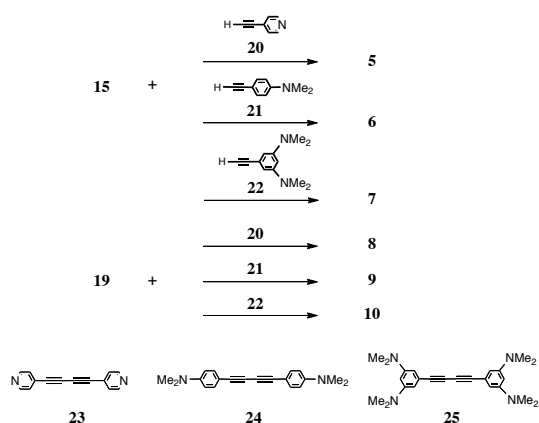
2.1. Synthesis of The OEP-SPC-LB Derivatives 5-10.

The title OEP-SPC-LB derivatives **5-10** were synthesized, as shown in **Schemes 1** and **2**.^{8,11} The counterparts of terminal OEP-SPC acetylenes **15** and **19** were prepared by our conventional way. Oxidative cross coupling reactions of the OEP acetylene **11**¹⁶ with the ethynyl compounds **12**¹⁷ and **16**¹⁸ were carried out under the modified Eglinton conditions in ordinary yields,¹⁹ followed by ethynylation of the bromo substituent of **13** and **17** with trimethylsilylacetylene (TMS-acetylene) by Sonogashira coupling reaction and alkaline hydrolysis.²⁰ Then, the derivatives **5-10** were led, again by Eglinton cross coupling reaction of **15** or **19** with the respective LB acetylenes **20**,²¹ **21**,²¹ and **22**.²¹ The reaction of **15** with an excessive amount (ca. 10 eq. to **15**) of **20**, **21**, or **22** was carried out in a mixture of Py and methanol (MeOH) (5:1 in v/v) in the presence of copper(II) acetate [Cu(OAc)₂]. In general, the reaction mixtures were chromatographed on

silica-gel (SiO₂) column, to afford the desired products **5**, **6**, and **7** in 25-45% yields, together with the corresponding homo-coupling dimers **23**,²² **24**,²³ and **25**¹¹ in quantity. Similarly, the reactions of **19** with **20-22** gave the corresponding **8**, **9**, and **10** in similar yields to those of **5-7**. All the highly extended π -electronic conjugated OEP derivatives **5-10** are dark green to black purple microcrystallines and are stable under the room light at an ambient temperature (see Experimental part).



Scheme 1. Preparation of the terminal acetylenes **15** and **19** of OEP-SPC.



Scheme 2. Synthesis of OEP-SPC-LB **5-10** by the oxidative coupling reactions of **15** or **19** with the LB terminal acetylenes **20-22** and their homo-coupling products **23-25**.

2.2. Molecular Skeletal and Electronic Structural Features of OEP-SPC-LB from ¹H NMR, IR, and UV-Vis Spectral Measurements.

All the ¹H NMR spectra of OEP-SPC-LB **5-10** are almost comparable to the simply combined ones between corresponding components (**S1**), similar to those of **1-4**.¹⁵ Yet, all the H signals belonging to OEP and Anth of **10** appeared at almost the same chemical shifts as those of **8** and **9**, indicating that the connection of OEP, SPC, and LB components with the diacetylene linkage brings no particular reformation into their skeleton. Nevertheless, the H signals due to LB rings (LB-H) of **8-10** appeared in a slightly but apparently lower field region (~0.1 ppm), as compared with the corresponding LB-H of **5-7**, due to the greater diamagnetic ring current effect of the Anth SPC on these LB-H signals. Otherwise, this result suggests that the molecular planarity of the Anth derivatives **8-10** is higher and thus their π -electronic conjugation extends further than that of the Phen derivatives **5-7**, because the central Phen moiety of Anth in **8-10** is more fragile and mobile than Phen in **5-7** (vide infra). In other word, even if the central Phen moiety of Anth participates into π -electronic extension over the molecule more or less, the two more benzene rings substantially remain in the Anth component of **8-10**. Such a dibenzo-1,4-phenylene character of Anth magnetically affects those LB-H more intensively than one benzene ring of Phen in **5-7**.¹⁵

Similar to the above consequence from ¹H NMR spectra, IR spectral behavior would appear on the stretching vibrations due to the C-C triple (C::C) bond, reflecting the molecular planarity of this system. All the diacetylene linkages in the OEP-SPC-LB skeleton were practically observed, as a set of medium and weak absorption peaks (**Table 1**). The TT isomers of **1-4** showed the lower wave numbers, as compared with the corresponding HH isomers, indicating that the diacetylene linkage takes part in conjugation well with the higher planar SPC, though by a little.⁸ However, the reformation efficiency of the diacetylene linkage in this system is quite different between the OEP-SPC-LB derivatives. The C::C vibrations in a group of the DHBTh derivatives weaken largely in the order of LB; Py>DMAB>BisDMAB, while those in two groups of the Phen and Anth derivatives largely in the order of LB; DMAB>Py>BisDMAB, indicating an existence of some suggestive interaction between SPC and LB. It is hopefully expected that a combination between Anth and BisDMAB possesses the electronically highest transmission ability to OEP.

Table 1. The wave numbers (ν/cm^{-1}) due to the triple bond vibrations of OEP-SPC-LB measured by IR spectra (KBr disc)

OEP-SPC-LB	medium band	weak band
1_{HH}	2200	2130
1_{TT}	2196	2122
2_{HH}	2189	2131
2_{TT}	2184	2129
3_{HH}	2183	2130
3_{TT}	2178	2128
4_{HH}	2182	2132
4_{TT}	2178	2129
5	2188	2163
6	2202	2137
7	2175	2137
8	2173	2131
9	2180	2127
10	2168	2121

In contrast with a fairly high similarity in the molecular skeletal features, the electronic absorption spectral behaviors in a region of 400-600 nm, characteristic of OEP nucleus,^{13b, 14} are affected dramatically by the nature of SPC (**Fig. 1**). A set of **4_{HH}** and **4_{TT}** is a typical example, where the greater extension of π -electronic conjugation over the molecule is performed in **4_{TT}** due to the higher planarity of TT-DHBTh effective for π -electronic conjugation.¹¹ On the other hand, the Phen derivative **7** showed almost the same spectrum as **4_{HH}** in both absorption maxima and intensity, clearly indicating that the transmissible ability of SPC from LB to OEP in this system is almost identical between Phen and HH-DHBTh (vide infra).

As compared with the spectral behaviors of the DHBTh and Phen derivatives, the Anth derivative **10** exhibited much drastic changes in both Soret and Q bands. The much further reformation of electronic structure of OEP was achieved, affording the completely separated Soret band with two clear maxima and the much sharper Q band at the longer wavelength region. The connection mode of **9** and **10** positions of Anth would be also important for the more efficient reformation of the electronic structure of OEP, as observed in the diacetylene-group connected OEP-Anth-OEP derivatives.¹⁵ In particular, with respect to the longer wavelength Q band, the absorption intensity of **10** proved to increase up to $\epsilon=37500$, almost twice and three times as large as that of **4_{TT}** and **7**, which is of significance for development of the OEP chromatic system in both sensitivity and visibility.

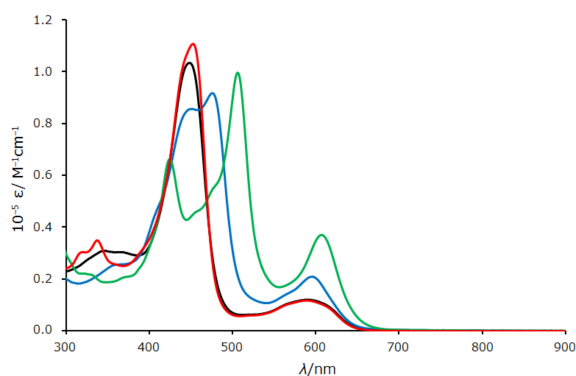


Figure 1. Electronic absorption spectra of **4_{HH}** (black), **4_{TT}** (blue), **7** (red), and **10** (green) (in CHCl_3 , 25 °C).

In order to seek some structural element at the molecular level, the HOMO and LUMO energies were preliminarily calculated for the SPC-LB derivatives **26-37** (Chart 6) with a program of PM7 level and were summarized in Table 2.²⁴ It largely shows that the HOMO energies elevate in the order of LB; Py<DMAB<BisDMAB, while the LUMO energies lower in the order of LB; DMAB>BisDMAB>>Py. Consequently, in all sets of derivatives with the same LB, the gaps (Δ) between HOMO and LUMO decreased in the order of SPC; Phen>HH-DHBTh>TT-DHBTh>Anth, resulting in the largest (8.3611 eV) for **32** and the smallest (6.6792 eV) for **37**. These results indicate that the combination of Phen and Py is the hardest to collapse their electronic structures, while the combination of Anth and BisDMAB is the easiest for reformation of their electronic structures to enter into an extended conjugation system through the diacetylene linkage.²⁵ This is exactly in accord with the empirical results from the C::C bond vibrations of OEP-SPC-LB (vide supra).

Table 2. HOMO and LUMO energies (eV) of diacetylene-group connected SPC-LB derivatives **26-37**

SPC-LB	HOMO	LUMO	Δ (HOMO - LUMO)
26	-8.8910	-1.3290	7.5620
27	-8.0660	-0.9000	7.1660
28	-8.0410	-0.9580	7.0830
29	-8.7570	-1.3840	7.3730
30	-8.0230	-1.0260	6.9970
31	-8.0250	-1.0630	6.9620
32	-9.3767	-1.0156	8.3611
33	-8.1457	-0.4485	7.6972
34	-8.0320	-0.4980	7.5340
35	-8.4060	-1.6420	6.7640
36	-8.0620	-1.3060	6.7560
37	-8.0440	-1.3648	6.6792

Molecular orbital calculation was performed by a program of PM7 level (MOPAC2012)^{24b, c} together with optimization of each molecular structure with a Winmoster program.^{24a}

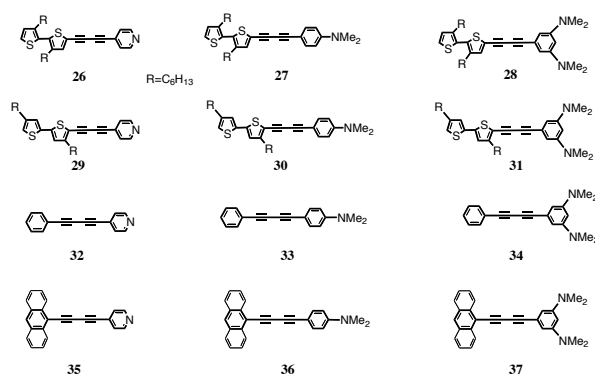


Chart 6. Diacetylene-group connected SPC-LB derivatives **26-37**.

Based on the fact that the Phen and Anth derivatives **5-10** are more compact molecules in conjugation length than the DHBTh derivatives **1-4**, it suggests that an introduction of the mobile π -electronic component into the present system is much preferable to a canonical extension of the π -electronic conjugation, for construction of the particular electronic structure of OEP as an acid-sensing material of this type.

2.3. The Spectral Behavior of OEP-SPC-LB Under The Acidic Conditions and Cooperative Effect of SPC and LB on Their Spectral Changes.

2.3.1. ¹H NMR Spectral Changes. All the experiments were achieved under the same conditions as previously reported for **1-4**.¹¹ As seen in the spectral changes of **5** (Fig. 2), **6** (S2) and **7** (S3), on increasing TFA content in each sample solution, the signals due to LB-H regularly shift to the lower field at the first stage more or less until they reach to the equilibrium state, because the positive charge is introduced into LB ring by protonation on its N atom and thus magnetically deshields LB-H. Further addition of TFA suddenly starts to broaden the meso-H signals with their chemical shifts unchanged and finally makes them hide into the base line.⁸ Although the amounts of TFA necessary for completion of those spectral changes are different from each other, the Phen derivatives **5-7** substantially showed the similar behavior to the DHBTh derivatives **1-4**.¹¹ Also, it should be noted that all the Phen-H signals in **5-7** remain unchanged in both neutral and acidic media, similar to the DHBTh-H signals of **1-4**.⁸

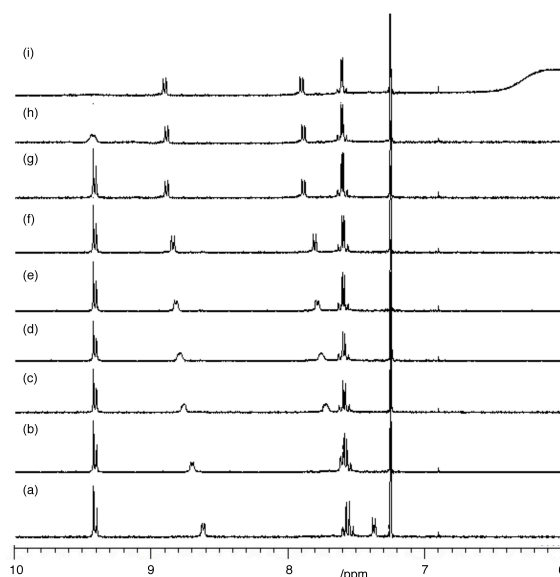


Figure 2. ¹H NMR spectral changes of **5** in a range of 6-10 ppm with adding TFA to the CDCl_3 sample: (a) 0 equiv, (b) 1 equiv, (c) 2 equiv, (d) 3 equiv, (e) 4 equiv, (f) 5 equiv, (g) 10 equiv, (h) 15 equiv, and (i) 20 equiv to **5**.

In contrast with a high regularity in TFA-response between the Phen derivatives **5-7**, the Anth derivatives **8-10** exhibited the characteristic behavior, with reflection of the nature of LB. The Py-H signals of **8** (δ 8.69 and 7.47 ppm) scarcely shifted to the lower field but unexpectedly moved toward the higher field to reach the final stationary positions at ca. 8.1 and ca. 7.2 ppm (Fig. 3). This is entirely reverse to the behavior of the Py-H signals of **1** and **5**. Yet, all the Anth-H signals were also observed to move toward the higher field and were almost independently positioned from each other at the end. The DMAB-H signals (δ 7.51 and 6.66 ppm) of **9** once shifted to the lower field (δ 7.55 and ca. 7.0 ppm) but on further addition

of TFA reversely shifted to the higher field just by a little (S4). And, only a set of the Anth-H signals near by the diacetylene linkage moved toward the higher field from beginning to end. In the case of **10** (Fig. 4), the BisDMAB-H signals (δ 6.45 and 6.12 ppm) did not exhibit a typical movement arising from its diacid base property, distinct from **4** and **7**,¹¹ but simply shifted to the lower field (δ ca. 7.1 and ca. 7.0 ppm). Yet, quite similar to the behavior of **9**, only a set of the Anth-H signals near by the diacetylene linkage shifted to the higher field. With respect to the meso-H signals, no particular difference between these Phen and Anth derivatives was observed in spectral changes.

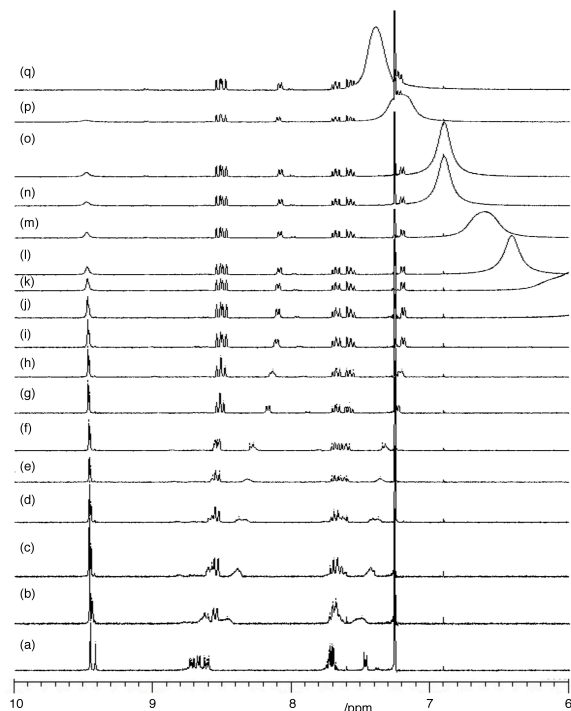


Figure 3. ^1H NMR spectral changes of **8** in a range of 6-10 ppm with adding TFA to the CDCl_3 sample: (a) 0 equiv, (b) 1 equiv, (c) 2 equiv, (d) 3 equiv, (e) 4 equiv, (f) 5 equiv, (g) 10 equiv, (h) 15 equiv, (i) 20 equiv, (j) 25 equiv, (k) 30 equiv, (l) 35 equiv, (m) 40 equiv, (n) 45 equiv, (o) 50 equiv, (p) 55 equiv, and (q) 60 equiv to **8**.

It is apparent that such a big difference of **8-10** from the derivatives **1-7** in their spectral behavior in acidic media is attributable to the high π -electron mobility of Anth and cooperatively to its interactive efficiency with LB, as also suggested from the stretching vibrations of C::C bond in their IR spectral study (vide supra). Under the acidic conditions, the mono-protonated LB species (LBH^+) must be stabilized somehow, because the positive charge is introduced into the OEP-SPC-LB skeletal system (Charts 3 and 4). In the case of **8**, the positive charge of PyH^+ would localize on the N atom of Py to have the strong electron-withdrawing power, because of no charge relaxation through the π -electronic conjugation with any π -electronic components. In contrast with PyH^+ , the positive charge of DMABH^+ (**9**) and BisDMABH^+ (**10**) would have the weak electron-withdrawing power, because these species delocalize their positive charge for stabilization. Therefore, the difference in electronically inductive power between these mono-protonated species likely affects the π -electron mobility of Anth more or less, according to circumstances. For example, the PyH^+ intensively induces Anth to collapse its 14 π -electron ring system by withdrawing π -electrons to the PyH^+ site and to reduce its ring current effect to some extent. Oppositely, the PyH^+ ring increases the electron density by accepting π -electrons from the Anth site, resulting in

shielding the protons of the PyH^+ ring to some extent. Thus, the π -electronic reformation of this type would induce both Anth-H and Py-H signals to shift to the higher field.

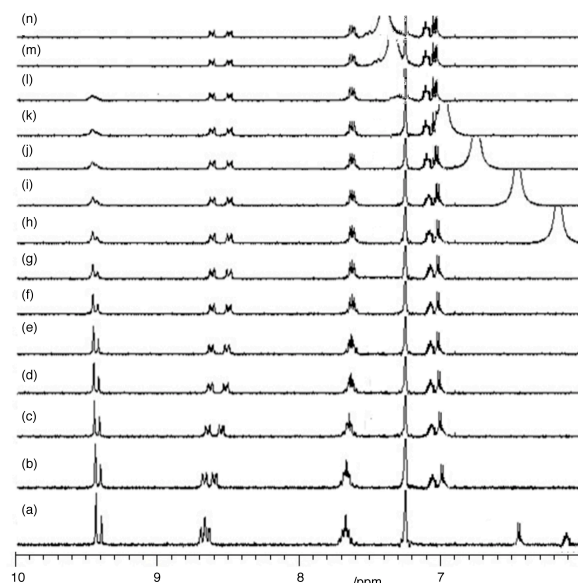


Figure 4. ^1H NMR spectral changes of **10** in a range of 6-10 ppm with adding TFA to the CDCl_3 sample: (a) 0 equiv, (b) 1 equiv, (c) 2 equiv, (d) 3 equiv, (e) 4 equiv, (f) 5 equiv, (g) 10 equiv, (h) 20 equiv, (i) 30 equiv, (j) 40 equiv, (k) 50 equiv, (l) 60 equiv, (m) 80 equiv, and (n) 100 equiv to **10**.

As a result, it is experimentally verified that the π -electron mobility of SPC plays an important role not only in the purposive construction of the skeletal feature of this system, but also in the transmissible efficiency of this system from LB to OEP through the diacetylene linkage under both neutral and acidic conditions.

2.3.2. Electronic Absorption Spectral Changes.

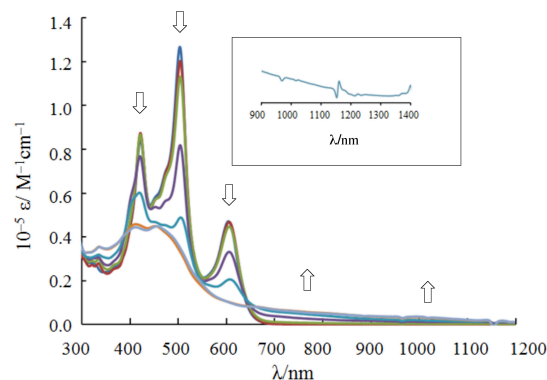


Figure 5. Electronic absorption spectral changes of **10** (ca. 2.5×10^{-5} mol L^{-1}) with TFA content to **10** in the CHCl_3 sample; 0 equiv. (dark blue), 1×10^3 equiv. (brown), 4×10^3 equiv. (green), 1×10^4 equiv. (purple), 4×10^4 equiv. (blue), 8×10^4 equiv. (orange), and 1×10^5 equiv. (light blue) to **10**. Arrows show the intensity change of each absorption band with increasing TFA content. The inset shows the absorption tailing over 1400 nm.

All the experiments were achieved under the same conditions as previously reported for **1-4**.¹¹ Generally, on adding TFA into the sample solution, Soret and Q bands of all the derivatives regularly decrease their intensity at first, and then both bands start to deform their shapes from the certain point of TFA content in the sample, accompanied by a new absorption band at the longer wavelength with a long tail. As contrasted with the absorption terminal (\sim ca. 900 nm) of the derivatives **1-7**, those of **8-10** extended over the visible region

up to ca. 1200-1400 nm (Figs. 1 and 5). In accord with these spectral changes, the derivatives change their solution-color appearance, mostly from greenish to pale yellow for the DHBTh derivatives 1-4 at the end (Fig. 6a-c). This is almost the same change in color for all the Phen derivatives 5-7.²⁷ And, the Anth derivatives 8-10 exhibited much wider solution-color change from greenish to reddish at the end (Fig. 6d-f).

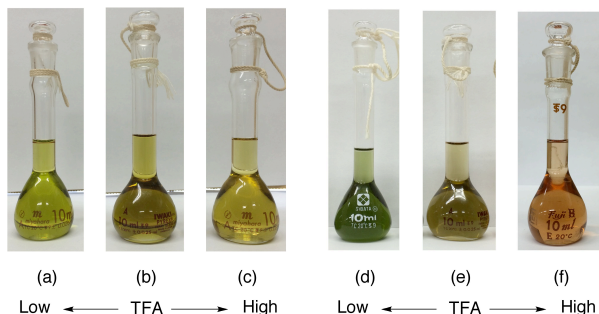


Figure 6. Solution-color changes of the CHCl₃ samples with adding TFA: (a)-(c) for **2_{HH}** and (d)-(f) for **10**.

As shown from the ¹H NMR and IR spectral experiments, it is realized that the Anth SPC works cooperatively with LB in high efficiency and possesses a remarkable influence on the electronic absorption spectral behavior of **8-10** also under the acidic conditions (see the next section).

2.3.3. Sensitivity, Stability, and Visibility to TFA.

In this study, the minimum amount of TFA necessary for completion of the mono-protonation onto LB is regarded as a measure of sensitivity to TFA; the less value means the higher sensitivity.¹¹ On the other hand, in general, the metal complexes of porphyrin are labile under the acidic conditions to extrude the metal ions (Chart 3).^{13, 28} Therefore, in order to guarantee the reversibility between neutral and acidic media in the spectral changes, the minimum amount of TFA necessary for completion of the meso-H signal disappearance was employed,¹¹ correlating the greater value with the higher reversible stability (Table 3).

In a group of OEP-SPC-Py, both DHBTh and Anth derivatives **1** and **8** showed almost the same sensitivity, to be ca. 10 times as sensitive as the Phen derivative **5**. In a group of OEP-SPC-DMAB, the Anth SPC derivative **9** showed the highest sensitivity, to be ca. 7 times as sensitive as the DHBTh derivative **2** and 10 times as sensitive as the Phen derivative **6**. And, in a group of OEP-SPC-BisDMAB, all the derivatives **4**, **7**, and **10** showed the fairly high sensitivity, regardless of SPC, exactly due to a high proton-acceptable ability of BisDMAB. In particular, a combination between Anth and BisDMAB brought the highest sensitivity, as also expected in their IR and electronic spectral studies (Tables 1-3). On the other hand, among the derivatives carrying the same LB, the Anth group mostly proved to show the higher reversible stability than the other DHBTh and Phen groups. In particular, the OEP-Anth-BisDMAB derivative **10** possesses the reversibility 32 times as stable as the OEP-DHBTh-Py derivative **1**. Meantime, the reversible stability of the Phen derivatives **5-7** showed an irregular trend, depending on the LB component. As compared with the corresponding DHBTh derivatives **1-4**, the Py derivative **5** was more stable than **1**, the DMAB derivative **6** was stable similar to **2**, and the BisDMAB derivative **7** was less stable than **4** (vide infra).

Table 3. Minimum amount of TFA necessary for completion of the respective step processes in the OEP-SPC-LB system examined by means of ¹H NMR spectral measurements

OEP-SPC-LB	Added TFA (equiv.)	
	1st step	2nd step
1_{TT}	1.1	2.5
2_{TT}	10	25
3_{TT}	5.0	35
4_{TT}	1.5	60
5	10	20
6	15	25
7	1.0	25
8	1.2	60
9	1.5	60
10	1.0	80

All experiments were carried out at 25 °C using the sample solutions adjusted to the concentration of ca. 8.5 × 10⁻³ mol/10³ cm³. The 1st step is for completion of the mono-protonation onto LB and the 2nd step is for completion of the disappearance of meso-H signals.

At this moment, it is hard to make a general rationale of sensitivity and stability of this system quantitatively, but the acid-base interaction principle somewhat throws a light on the above results. Thus, at the first stage, the sensitivity correlates with the higher electron-donating ability of LB to TFA or with the more localized electrons on the N atom of LB. Simultaneously, when the N-protonated species of LB formed at the first stage can stabilize sufficiently by relaxation of its positive charge somehow (Chart 4), the protonation onto LB would take place efficiently with the less amount of TFA than otherwise. At the second stage, such thermodynamically higher stability of the conjugated acid, OEP-SPC-LBH⁺, would reversely retard the acid-base reaction of its OEP component with TFA, and thus need the greater amount of TFA for completion of the meso-H signal disappearance (vide supra). Thus, the stability of the present system decisively reflects the thermodynamical stability of OEP-SPC-LBH⁺ (Chart 3).

As mentioned previously, the lone pair electrons of Py reside on N atom stubbornly in an sp²-hybridized orbital, while those of DMAB and BisDMAB partially take part in π-electronic conjugation (Chart 4). Accordingly, Py would show the higher basicity and thus would possess the higher sensitivity than DMAB and BisDMAB. Table 3 also shows a particular contribution to the basicity in BisDMAB, affording a high sensitivity of **4** and **10** almost comparable to that of **1** and **8**. This result probably comes from a strong assistance of the non-protonated amino group in BisDMAB, not only toward the on-going protonated amino group for enhancement of proton-acceptable ability but also toward the already protonated amino group for enhancement of thermodynamical stability.¹¹

In addition to the lone pair electrons on the N atom of LB, the π-electron mobility of SPC would play a significant role in not only sensitivity but also stability, reflecting the difference in efficiency of the π-electron supply from SPC to LB. In this situation, for example, the resonance energy of SPC could be regarded as a measure of efficiency in the π-electron supply from SPC; Phen moiety of Anth<3HTH of DHBTh<Phen.²⁹ The SPC with the smaller resonance energy would provide its π-electron more readily to the necessitated sites through an extension of the π-electronic conjugation, to heighten the basicity of LB under the neutral conditions and to enhance the thermodynamical stability of LBH⁺ under the acidic conditions. As deduced from a low sensitivity and stability of **5-7**, it is indicated that the Phen itself is much hard to collapse the 6π-electron ring system for an extension of the π-electronic

conjugation due to its greater resonance energy, as compared with other SPC. In case of the DHBTh derivatives **1-4**, their behavior seems variable. The fact that they carry two 3HTH rings with the medium resonance energy may result in a characteristic behavior in both sensitivity and stability, distinct from other SPC derivatives. Each 3HTH ring of DHBTh likely plays an independent role as the π -electron-provider component to enhance the basicity of the nearby LB or OEP ring, and to increase the thermodynamical stability of their conjugated acids (LBH⁺ or H⁺OEP), according to circumstances (**Chart 7**).

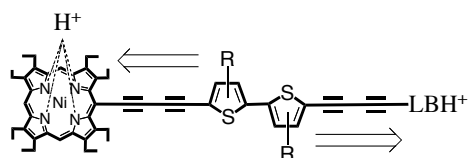


Chart 7. Independent interaction of each 3HTH ring in DHBTh on the nearby component OEP or LB through the diacetylene linkage.

From the results on the structure-property relationships in the OEP-SPC-LB system, it is simply noted that the combination between the higher basic LB and the lower resonance energy SPC is useful for further enhancement of the sensitivity and stability. In this respect, the OEP-Anth-BisDMAB derivative **10** proved to be the most promising candidate at present for the OEP chromatic system with highly reversible spectral changes between neutral and acidic media.

3. Conclusion

In this study, the features of our original OEP-SPC-LB chromatic system in reversible spectral change between neutral and acidic media were further elucidated in view of sensitivity, stability, and visibility, as focused on the electronic properties of LB and SPC. It was studied on their structural properties that the lone pair electrons on the N atom of LB interact with TFA strongly or weakly, depending on the circumstances where they take part in π -electronic conjugation for stabilization in an extended system or in a definite cyclic system. This feature primarily produces the inherent basicity of LB in the present system and results in the difference in their sensitivity to TFA. The π -electron mobility of SPC also plays a significant role for π -electronic conjugation with LB through the diacetylene linkage to reform the electronic structures, resulting in the difference in their reactivity with TFA. Simultaneously, these electronic properties of LB and SPC contribute to the stabilization of the conjugated acids under the acidic conditions as well. The higher basic LB derivatives did not always exhibit the higher reversible stability, but the SPC derivatives with the higher π -electron mobility certainly brought the higher sensitivity and stability (**Table 3**). In this respect, the Phen moiety of Anth proved to be the most effective SPC for the present system, presumably due to the smallest loss of resonance energy for reformation of the electronic system to provide its π -electrons to the necessitated sites. Especially, the combination between Anth and BisDMAB is highly promising for the OEP chromatic system in view of the three valuations of sensitivity, stability, and visibility.

A wide variety of porphyrin-based chromatic systems are well known to demonstrate one or two particular valuations with the same efficiency as **10** or more efficiently.³ Our OEP chromatic system is rather independent from others not only in aiming at all the three valuations based on the same molecular

skeleton, but also in performing them systematically and simply by incorporation of SPC and LB with its skeletal features remaining. Based on the guideline of molecular design derived from the present study, further investigations of the OEP derivatives composed of the higher π -electron mobile SPC and the more basic LB are now in progress.

4. Experimental

EI and FAB mass spectra were recorded with a JEOL JMS-700 spectrometer. IR spectra were measured on a Jasco FT/IR 7300 spectrophotometer as KBr or nujol or neat disk sample; only significant absorptions are recorded in ν values (cm^{-1}). ¹H NMR spectra were measured in CDCl₃ solution on a JEOL ECX-300A (300 MHz) or a JEOL JMN-EPC 600 (600 MHz) spectrometer and were recorded in δ values (ppm) with TMS as an internal standard. The coupling constants (*J*) are given in Hz. Similarly, ¹³C NMR spectra were measured on a JEOL JMN-EPC 600 (150 MHz) spectrometer, in which their signals were not satisfactorily assigned to each carbon yet. Electronic absorption spectra were measured in CHCl₃ solution on a Shimadzu UV-2200A spectrophotometer and absorption maxima of respective bands are reported in λ_{max} (nm) values together with their molecular extinction coefficient (ϵ) and note (sh; shoulder). SiO₂ (Fujisilysia BW 820MH or BW 127ZH) was used for column chromatography. Reactions were followed by TLC, on aluminum sheets pre-coated with Merck SiO₂ F₂₅₄ or with Merck Al₂O₃ GF₂₅₄. Organic extracts were dried over anhydrous sodium sulfate (Na₂SO₄) or magnesium sulfate (MgSO₄) prior to removal of the solvents.

According to the literatures, the OEP terminal acetylenes of **15** and **19** as counterparts for OEP-SPC-LB were prepared, according to our conventional way.^{8,11}

Preparation of the diacetylene-group connected OEP-phenylacetylene **15**: To a solution of Cu(OAc)₂ (5.34 g, 29.4 mmol) in Py-MeOH (120 cm³, 5:1) was added the mixture of **11**¹⁶ (600 mg, 0.97 mmol) and **12**¹⁷ (619 mg, 3.42 mmol) in Py-MeOH (240 cm³, 5:1) at 40-45 C over 12h and was stirred there for 1d. Poured into water, the reaction mixture was extracted with CHCl₃. The extracts were washed with dil. HCl, sat. NaHCO₃, and brine successively, and then dried. The residue obtained after removal of the solvent was chromatographed on SiO₂ (3 x 30 cm) with hexane-CHCl₃ (1:4) to afford **13** (248 mg, 32%) as dark green microcrystallines. **13**: MS (EI); *m/z* 793 (M⁺) and 795 (M⁺+2) for C₄₆H₄₇N₄BrNi (MW 794.47, based on Ni=58.69). IR (KBr) ν 2961, 2926, and 2866 (CH) and 2199 and 2137 (C:::C). ¹H NMR; δ 9.42 (2H, s, meso-H), 9.40 (1H, s, meso-H), 7.52 (2H, d, *J* 8.4, Phen-H), 7.47 (2H, d, *J* 8.4, Phen-H), 4.13 (4H, q, *J* 8.3, CH₂), 3.85-3.75 (12H, m, CH₂), and 1.83-1.70 (24H, m, CH₃). ¹³C NMR; δ 145.79, 145.00, 143.77, 143.01, 142.21, 140.34, 140.16, 137.75, 133.70, 131.77, 123.43, 121.41, 97.90, 97.84, and 92.29 (sp²-C), 90.80, 87.31, 82.14, and 76.00 (sp-C), 31.94, 29.72, 29.67, 22.70, 21.77, 19.50, 18.14, and 17.27 (sp³-C). Uv-vis; λ_{max} 437 (110000), 565 (13100), and 603 (13700). To a solution of **13** (150 mg, 0.19 mmol), (Ph₃P)₄Pd (436 mg, 3.8 x 10⁻² mmol), and CuI (3.6 mg, 1.9 x 10⁻² mmol) in toluene-NET₃ (30 cm³, 1:1) was added TMS-acetylene (0.11 cm³, 0.76 mmol) over 3h. The mixture was refluxed with stirring for 12 h. The reaction mixture was poured into water and extracted with CHCl₃. The extracts were washed with brine and then dried. The residue obtained after removal of the solvents was chromatographed on SiO₂ (3.5 x 24 cm) with hexane-CHCl₃ (4:1) to afford **14** (123 mg, 80%) as black purple microcrystallines. **14**: MS (EI); *m/z* 811 (M⁺) for C₅₁H₅₆N₄NiSi (MW 811.78, based on Ni=58.69). IR (nujol) ν 2962, 2927, and 2869 (CH) and 2193 and 2136 (C:::C). ¹H NMR; δ 9.42 (2H, s, meso-H), 9.40 (1H, s, meso-H),

7.53 (2H, d, *J* 7.8, Phen-H), 7.46 (2H, d, *J* 7.8, Phen-H), 4.13 (4H, q, *J* 8.2, CH₂), 3.85-3.75 (12H, m, CH₂), 1.83-1.70 (24H, m, CH₃), and 0.27 (9H, s, TMS-H). ¹³C NMR; δ 146.29, 145.53, 144.27, 143.51, 142.69, 140.84, 140.64, 138.24, 134.21, 132.63, 124.19, 122.91, 98.33, 97.73, and 92.79 (sp²-C), 91.29, 88.49, 87.81, 83.03, 82.62, and 76.49 (sp-C), 30.21, 22.26, 20.05, 20.00, 19.97, 18.65, 17.78, and 0.51 (sp³-C). One sp³-C signal could not be ascertained, implying that the signal possesses the same chemical shift as the firmly specified one. Uv-vis; λ_{max} 441 (112000), 568 (9120), and 608 (9400). A mixture of **14** (151 mg, 0.19 mmol) and K₂CO₃ (13 mg, 9.3 x 10⁻² mmol) in CHCl₃-MeOH (30 cm³, 1:1) was stirred at an ambient temperature under Ar atmosphere for 6 h. Poured into water, the reaction mixture was extracted with CHCl₃. The extracts were washed with brine and then dried. The residue obtained after removal of the solvents was chromatographed on SiO₂ (5 x 8.0 cm) with CHCl₃ to afford **15** (137 mg, quantitative) as dark purple microcrystallines. **15**: MS (EI); *m/z* 739 (M⁺) for C₄₈H₄₈N₄Ni (MW 739.59, based on Ni=58.69). IR (KBr) ν 3293 (C:::CH), 2961, 2925, and 2854 (CH), and 2193 and 2136 (C:::C). ¹H NMR; δ 9.42 (2H, s, meso-H), 9.40 (1H, s, meso-H), 7.55 (2H, d, *J* 8.7, Phen-H), 7.47 (2H, d, *J* 8.7, Phen-H), 4.13 (4H, q, *J* 7.2, CH₂), 3.84-3.74 (12H, m, CH₂), 3.18 (1H, s, C:::CH), and 1.84-1.72 (24H, m, CH₃). ¹³C NMR; δ 145.80, 145.06, 143.76, 143.00, 142.31, 140.40, 140.21, 137.83, 132.21, 132.16, 122.97, 122.73, 97.93, 97.87, and 92.38 (sp²-C), 90.91, 87.81, 83.19, 82.65, 79.48, and 76.79 (sp-C), 32.02, 29.79, 21.82, 20.68, 19.58, 19.50, 18.15, and 17.28 (sp³-C). Uv-vis; λ_{max} 443 (99700), 567 (7930), and 608 (8300).

Preparation of the diacetylene-group connected OEP-Anthrylacetylene **19**: To a solution of Cu(OAc)₂ (5.18 g, 28.7 mmol) in Py-MeOH (120 cm³, 5:1) was added the mixture of **11**¹⁶ (600 mg, 0.97 mmol) and **16**¹⁸ (960 mg, 3.42 mmol) in Py-MeOH (240 cm³, 5:1) at 40-45 C over 6 h and was stirred there for 12 h. Poured into water, the reaction mixture was extracted with CHCl₃. The extracts were washed with dil. HCl, sat. NaHCO₃, and brine successively, and then dried. The residue obtained after removal of solvent was chromatographed on SiO₂ (3 x 27 cm) with hexane-CHCl₃ (4:1) to afford **17** (288 mg, 33%) as dark green microcrystallines. **17**: MS (FAB); *m/z* 894.56 (M⁺) for C₅₄H₅₁N₄BrNi (MW 894.58, based on Ni=58.69). IR (KBr) ν 2961, 2927, and 2868 (CH), and 2180 and 2128 (C:::C). ¹H NMR; δ 9.44 (2H, s, meso-H), 9.40 (1H, s, meso-H), 8.70 (2H, dm, Anth-H), 8.57 (2H, dm, Anth-H), 7.70-7.63 (4H, m, Anth-H), 4.28 (4H, q, *J* 7.5, CH₂), 3.87-3.75 (12H, m, CH₂), 1.94 (6H, t, *J* 7.8, CH₃), and 1.78-1.73 (18H, m, CH₃). ¹³C NMR; δ 145.86, 144.89, 143.75, 142.99, 142.26, 140.36, 140.18, 140.06, 137.79, 133.90, 130.26, 128.39, 127.55, 127.04, 125.23, 117.25, 97.98, 97.87, and 92.73 (sp²-C), 91.07, 86.94, 85.49, and 85.46 (sp-C), 31.93, 29.71, 29.37, 21.89, 19.53, 19.47, 18.16, and 17.48 (sp³-C). Uv-vis; λ_{max} 414 (66300), 448 (78300), 482 (99800), 565 (14900, sh), and 598 (22400). To a solution of **17** (150 mg, 0.17 mmol), (Ph₃P)₄Pd (39.1 mg, 3.4 x 10⁻² mmol), and CuI (3.5 mg, 18.4 x 10⁻² mmol) in toluene-TEA (30 cm³, 2:1) was added TMS-acetylene (0.1 cm³, 0.72 mmol) and the mixture was refluxed with stirring for 12 h. The reaction mixture was poured into water and extracted with CHCl₃. The extracts were washed with brine and then dried. The residue obtained after removal of the solvent was chromatographed on SiO₂ (3.5 x 21 cm) with hexane-CHCl₃ (4:1) to afford **18** (128 mg, 84%) as black purple microcrystallines. **18**: MS (FAB); *m/z* 911.95 (M⁺) for C₅₉H₆₀N₄SiNi (MW 911.92, based on Ni=58.69). IR (KBr) ν 2962, 2928, and 2869 (CH) and 2176 and 2134 (C:::C). ¹H NMR; δ 9.45 (2H, s, meso-H), 9.41 (1H, s, meso-H), 8.74-8.68 (2H, m, Anth-H), 8.64-8.59 (2H, m, Anth-H), 7.73-7.63 (4H, m,

Anth-H), 4.26 (4H, q, *J* 7.5, CH₂), 3.88-3.76 (12H, m, CH₂), 1.94 (6H, t, *J* 7.2, CH₃), 1.80-1.74 (24H, m, CH₃), and 0.45 (9H, s, TMS-H). ¹³C NMR; δ 145.69, 144.78, 143.58, 142.83, 142.09, 140.17, 139.99, 137.60, 133.61, 133.48, 132.81, 132.14, 128.51, 128.32, 128.27, 127.28, 127.12, 101.31, and 97.81 (sp²-C), 92.69, 90.93, 87.33, 85.81, and 85.69 (sp-C), 21.69, 19.35, 19.28, 17.97, 17.95, 17.18, and 0.05 (sp³-C). One sp-C and two sp³-C signals could not be ascertained, implying that their signals possess the same chemical shift as the firmly specified one (ones). In order to specify those signals, the ¹³C NMR spectra will be taken in other solvents in the future. Uv-vis; λ_{max} 419 (77400), 440 (61100, sh), 465 (66300), 491 (100000), 563 (16200), and 601 (29400). A solution of **18** (170 mg, 0.20 mmol) and K₂CO₃ (12.9 mg, 9.3 x 10⁻² mmol) in CHCl₃-MeOH (30 cm³, 1:1) was stirred at an ambient temperature under Ar atmosphere for 10 h. Poured into water, the reaction mixture was extracted with CHCl₃. The extracts were washed with brine and then dried. The residue obtained after removal of the solvents was chromatographed on SiO₂ (5 x 7.0 cm) with CHCl₃ to afford **19** (153 mg, 98%) as dark purple microcrystallines. **19**: MS (FAB); *m/z* 839.72 (M⁺) for C₅₆H₅₂N₄Ni (MW 839.71, based on Ni=58.69). IR (KBr) ν 3300 (C:::CH), 2962, 2923, and 2869 (CH), and 2174 and 2122 (C:::C). ¹H NMR; δ 9.45 (2H, s, meso-H), 9.42 (1H, s, meso-H), 8.72-8.69 (2H, dm, Anth-H), 8.69-8.64 (2H, dm, Anth-H), 7.73-7.64 (4H, m, Anth-H), 4.26 (4H, q, *J* 7.2, CH₂), 4.13 (1H, s, C:::CH), 3.86-3.76 (12H, m, CH₂), 1.96 (6H, t, *J* 7.2, CH₃), and 1.78-1.74 (24H, m, CH₃). ¹³C NMR; δ 145.91, 144.95, 143.80, 143.03, 142.29, 140.39, 140.19, 137.81, 132.93, 132.61, 132.10, 128.55, 127.35, 127.09, 118.14, 118.00, 98.02, 97.92, and 92.56 (sp²-C), 91.04, 90.35, 87.61, 85.93, 85.79, and 80.36 (sp-C), 31.97, 29.75, 22.45, 21.89, 19.55, 19.48, 18.17, and 17.37 (sp³-C). Uv-vis; λ_{max} 419 (93500), 437 (89600, sh), 456 (81500), 488 (93200), 563 (20800, sh), and 602 (32100).

Among LB counterparts **20-22** for OEP-SPC-LB, the LB acetylenes **20** and **21** are commercially available. Thus, the BisDMAB acetylene **22** was prepared from the corresponding bromo derivative, according to the reported procedures.²¹ To a solution of 1-bromo-3,5-bis(*N,N*-dimethylamino)benzene²¹ (500 mg, 2.06 mmol), (Ph₃P)₂PdCl₂ (40 mg, 57 x 10⁻³ mmol) and CuI (9.5 mg, 49.9 x 10⁻³ mmol) in TEA (20 cm³) was added TMS-acetylene (1.50 cm³, 10.8 mmol). The mixture was stirred with refluxing for 1 d. The reaction mixture was poured into water and extracted with ethyl acetate (AcOEt). The extracts were washed with brine and then dried. The residue obtained after removal of the solvent was chromatographed on Al₂O₃ (35 x 18 cm) with hexane-AcOEt (1:1) to afford the TMS-protected product (402 mg). Then, a solution of the crude solid and K₂CO₃ (430 mg, 3.1 mmol) in THF-MeOH (90 cm³, 1:2) was stirred at an ambient temperature under Ar atmosphere for 10 h. Poured into water, the reaction mixture was extracted with CHCl₃. The extracts were washed with brine and then dried. The residue obtained after removal of the solvents was chromatographed on Al₂O₃ (3 x 20 cm) with benzene to afford **22** (287 mg, 74%) as brownish oil. **22**:²¹ MS (EI); *m/z* 189 (M⁺+1) for C₁₂H₁₆N₂ (MW 188.27). IR (neat); ν 3314 (C:::CH) and 2110 (C:::C). ¹H NMR; δ 6.30 (2H, d, *J* 2.4, BisDMAB-H), 6.04 (1H, br t, *J* 2.4, BisDMAB-H), 2.93 (1H, s, C:::CH), and 2.92 (12H, s, NMe₂-H).

All the title OEP-SPC-LB derivatives **5-10** were synthesized, in a similar way for the DHBTh derivatives **1-4**.⁸ As a typical reaction procedure, the synthesis of **5** is described in the following. A mixture of **15** (80 mg, 0.11 mmol) and **20** (154 mg as HCl salt, 1.1 mmol, 10 eq. to **15**) in a mixed solution of Py-MeOH (150 cm³, 5:1) was added dropwise at 40-45 C with stirring into a solution of Py-MeOH (50 cm³, 5:1)

containing an excessive amount of Cu(OAc)₂ (728 mg, 4.0 mmol) over 1.5 hr. Then, the reaction mixture was kept stirring at 40 °C for 12 hr. Poured into water, the reaction mixture was extracted with CHCl₃. The extracts were washed with diluted HCl aq., with brine several times successively, and then dried. After removal of the solvents under reduced pressure, the residue obtained was chromatographed on SiO₂ column with hexane-CHCl₃ (4:1), to afford **5** (25 mg, 28%), together with the Py homo-coupling dimer **23**²² (38 mg, 34% based on **20**).

5: Dark purple microcrystallines (benzene-CHCl₃). MS (FAB); m/z 840.68 for C₅₅H₅₁N₅Ni (MW 840.70, based on Ni=58.69). IR (KBr); ν 2963, 2928, and 2870 (C-H), 2188 and 2163 (C≡C). ¹H NMR; δ 9.42 (2H, s, meso-H), 9.40 (1H, s, meso-H), 8.62 (2H, d, J 6.0, Py-H), 7.58 (2H, d, J 7.0, Phen-H), 7.53 (2H, d, J 7.0, Phen-H), 7.38 (2H, d, J 6.0, Py-H), 4.14 (4H, q, J 7.2, CH₂), 3.82-3.77 (12H, qm, CH₂), and 1.82-1.70 (24H, m, CH₃). ¹³C NMR; δ 149.92, 145.97, 144.87, 143.84, 143.04, 142.32, 140.44, 140.21, 137.82, 133.56, 132.81, 130.07, 125.96, 119.42, 116.52, 98.09, 98.03, and 92.77 (sp²-C), 90.83, 88.67, 86.81, 85.90, 85.81, 82.36, 81.18, and 78.57 (sp-C), 21.89, 19.55, 19.48, 18.19, 18.17, 18.15, 17.40, and 17.39 (sp³-C). Uv-vis; λ_{max} 452 (95000) and 592 (11600).

23²²: Colorless solid (benzene-hexane). ¹H NMR; δ 8.57 (4H, J 4.5, Py-H) and 7.31 (4H, J 4.5, Py-H).

6: 41% yield. Dark purple microcrystallines (benzene-CHCl₃). MS (FAB); m/z 882.77 for C₅₈H₅₇N₅Ni (MW 882.78, based on Ni=58.69). IR (KBr); ν 2958, 2927, and 2868 (C-H), 2202 and 2137 (C≡C). ¹H NMR; δ 9.42 (2H, s, meso-H), 9.40 (1H, s, meso-H), 7.56 (2H, d, J 8.7, Phen-H), 7.49 (2H, d, J 8.7, Phen-H), 7.42 (2H, d, J 9.0, DMAB-H), 6.63 (2H, d, J 9.0, DMAB-H), 4.13 (4H, q, J 7.5, CH₂), 3.82-3.75 (12H, qm, CH₂), 3.01 (6H, s, NMe₂-H), and 1.83-1.73 (24H, m, CH₃). ¹³C NMR; δ 151.25, 145.78, 145.03, 143.74, 142.98, 142.22, 140.32, 140.13, 137.74, 133.91, 133.90, 132.25, 132.20, 123.05, 122.75, 116.65, 111.60, 97.90, and 97.82 (sp²-C), 87.88, 86.26, 85.84, 85.06, 83.15, 82.75, 78.15, and 72.35 (sp-C), 40.06, 21.76, 19.53, 19.46, 18.16, 18.13, 18.10, 17.25, and 17.20 (sp³-C). Uv-vis; λ_{max} 451 (131000) and 590 (14000).

24²³: 28% yield based on **21**. Pale yellow solid (benzene-hexane). ¹H NMR; δ 7.40 (4H, J 8.2, Phen-H), 6.64 (4H, J 8.2, Phen-H), and 2.98 (12H, s, NMe-H).

7: 35% yield. Black green powder (benzene-CHCl₃). MS (FAB); m/z 925.87 for C₆₀H₆₂N₆Ni (MW 925.85, based on Ni=58.69). IR (KBr); ν 2964, 2925, and 2870 (C-H), 2175 and 2137 (C≡C). ¹H NMR; δ 9.42 (2H, s, meso-H), 9.40 (1H, s, meso-H), 7.56 and 7.50 (2H and 2H, d, J 8.4, Phen-H), 6.35 (2H, br s, BisDMAB-H), 6.08 (1H, br s, BisDMAB-H), 4.13 (4H, q, J 7.2, CH₂), 3.82-3.77 (12H, qm, CH₂), 3.01 (12H, s, NMe₂-H), and 1.83-1.75 (24H, m, CH₃). ¹³C NMR; δ 145.80, 145.79, 145.00, 143.77, 143.01, 142.21, 140.34, 140.16, 137.75, 133.71, 133.70, 131.78, 131.77, 123.43, 121.41, 90.90, 97.84, 92.75, and 91.06 (sp²-C), 88.12, 88.10, 88.06, 87.58, 86.42, 86.17, 77.83, and 72.08 (sp-C), 40.68, 21.89, 19.55, 19.54, 19.48, 18.17, 18.15, 17.37, and 17.36 (sp³-C). Uv-vis; λ_{max} 450 (118000) and 590 (13500).

25¹¹: 45% based on **22**. Brownish solid (benzene). ¹H NMR; δ 6.34 (4H, d, J 2.4, BisDMAB-H), 6.07 (2H, t, J 2.4, BisDMAB-H), and 2.93 (24H, s, NMe₂-H).

8: 33% yield. Black purple powder (benzene-CHCl₃). MS (FAB); m/z 940.79 for C₆₃H₅₂N₅Ni (MW 940.81, based on Ni=58.69). IR (KBr); ν 2961, 2927, and 2868 (C-H), 2173 and 2131 (C≡C). ¹H NMR; δ 9.45 (2H, s, meso-H), 9.41 (1H, s, meso-H), 8.74-8.71 (2H, dm, Anth-H), 8.69 (2H, d, J 6.2, Py-H), 8.66-8.60 (2H, dm, Anth-H), 7.73-7.70 (4H, m, Anth-H), 7.47 (2H, d, J 6.2, Py-H), 4.26 (4H, q, J 7.5, CH₂), 3.86-3.76 (12H, qm, CH₂), 1.94 (6H, t, J 7.2, CH₃) and 1.79-1.74 (18H,

tm, CH₃). ¹³C NMR; δ 149.88, 145.86, 145.80, 144.97, 144.90, 143.81, 143.02, 142.22, 140.38, 140.17, 137.77, 137.70, 132.62, 132.60, 132.36, 132.30, 126.06, 123.89, 121.47, 97.97, 97.93, and 92.29 (sp²-C), 90.05, 89.05, 88.66, 87.90, 87.75, 83.38, 83.15, and 78.09 (sp-C), 21.76, 19.54, 19.47, 18.15, 18.14, 18.10, 17.27, and 17.20 (sp³-C). Uv-vis; λ_{max} 425 (91800), 508 (112000), and 610 (48700).

9: 40% yield. Black green powder (benzene-CHCl₃). MS (FAB); m/z 982.88 for C₆₆H₆₁N₅Ni (MW 982.89, based on Ni=58.69). IR (KBr); ν 2962, 2928, and 2869 (C-H), 2180 and 2127 (C≡C). ¹H NMR; δ 9.44 (2H, s, meso-H), 9.40 (1H, s, meso-H), 8.71-8.63 (4H, m, Anth-H), 7.71-7.62 (4H, m, Anth-H), 7.51 and 6.66 (2H and 2H, d, J 9.3, MDAB-H), 4.26 (4H, q, J 7.2, CH₂), 3.88-3.75 (12H, qm, CH₂), 3.02 (6H, s, NMe₂-H), 1.94 (6H, t, J 7.5, CH₃) and 1.79-1.74 (18H, tm, CH₃). ¹³C NMR; δ 150.75, 145.89, 144.97, 143.78, 143.01, 142.30, 140.38, 140.18, 137.80, 133.95, 133.22, 133.01, 127.47, 127.42, 127.24, 121.17, 118.57, 117.75, 111.71, 107.76, 98.02, 97.90, and 92.95 (sp²-C), 91.15, 88.26, 88.09, 87.91, 86.17, 86.16, 78.19, and 72.78 (sp-C), 40.08, 29.72, 29.71, 21.89, 19.55, 19.48, 18.19, 18.17, and 17.37 (sp³-C). Uv-vis; λ_{max} 425 (57900), 513 (88400), and 609 (41900).

10: 25% yield. Black green microcrystallines (benzene-CHCl₃). MS (FAB); m/z 1025.95 for C₆₈H₆₆N₆Ni (MW 1025.96, based on Ni=58.69). IR (KBr); ν 2963, 2927, and 2867 (C-H), 2168 and 2121 (C≡C). ¹H NMR; δ 9.45 (2H, s, meso-H), 9.41 (1H, s, meso-H), 8.70 and 8.65 (2H and 2H, dm, Anth-H), 7.73-7.66 (4H, m, Anth-H), 6.45 (2H, d, J 2.1, BisDMAB-H), 6.12 (1H, br s, BisDMAB-H), 4.26 (4H, q, J 7.2, CH₂), 3.86-3.76 (12H, qm, CH₂), 2.99 (12H, s, NMe₂-H), and 1.94 (6H, t, J 7.2, CH₃), 1.78-1.74 (18H, m, CH₃). ¹³C NMR; δ 151.43, 145.92, 144.95, 143.79, 143.02, 142.31, 140.40, 140.20, 137.81, 133.39, 132.97, 127.44, 127.40, 127.38, 127.21, 122.15, 118.21, 106.11, 98.86, 98.04, 97.94, 92.89, and 91.06 (sp²-C), 88.17, 88.10, 88.08, 87.61, 86.33, 86.05, 78.25, and 72.42 (sp-C), 40.68, 21.89, 19.55, 19.54, 19.47, 18.15, 18.14, 17.37, and 17.36 (sp³-C). Uv-vis; λ_{max} 426 (67900), 507 (99400), and 607 (37500).

Acknowledgement

Financial support by a Grant-in-Aid for Scientific Research from the Ministry of Education, Science, Sports, Culture and Technology (Nos. 23550046 and 26410039) is gratefully acknowledged. HH is also grateful to The Center of Instrumental Analyses at University of Toyama for their supporting measurements of physical properties of the new compounds.

Note: This paper is dedicated to an emeritus professor Soichi Misumi (Osaka University), on the occasion of his 90th birth-year anniversary.

References

- (a) Y.-L. Gong, F.-H. Li, F. Lu, C. Dai, *Bull. Mater. Sci.*, **2015**, 38, 847. (b) A. Quaranta, G. Charalambidis, C. Herrero, S. Margiola, W. Leibl, A. Coutsolelos, A. Aukauloo, *Phys. Chem. Chemical Phys.*, **2015**, 17, 24166. (c) S. Rangasamy, H. Ju, S. Um, D.-C. Oh, J. M. Song, *J. Med. Chem.*, **2015**, 58, 6864. (d) N. P. F. Goncalves, A. V. C. Simoes, A. R. Abreu, A. J. Abrunhosa, J. M. Dabrowski, M. M. Pereira, *J. Por. Phthal.*, **2015**, 19, 946.
- (a) R. H. Deibel, J. B. Evans, *J. Bacteriol.*, **1960**, 79, 356. (b) M. R. Dayer, A. A. Moosavi-Movahedi, M. S. Dayer, *Protein Peptide Lett.*, **2010**, 17, 473. (c) K. Komagoe, H. Kato, T. Inoue, T. Katsu, *Photochem. Photobiol. Sci.*, **2011**, 70, 363 and others.

3. (a) C.-G. Niu, X.-Q. Gui, G.-M. Zeng, A.-L. Guan, P.-F. Gao, P.-Z. Qin, *Anal. Bioanal. Chem.*, **2005**, 383, 349. (b) Y. Egawa, R. Hayashida, J. Anzai, *Langmuir*, **2007**, 23, 13146. (c) A. Synytsya, A. Synytsya, P. Blafkova, J. Ederova, J. Spevacek, P. Slepicka, V. Kral, K. Volka, *Biomacromol.*, **2009**, 10, 1067. (d) X. Zhu, W. Lu, Y. Zhang, A. Reed, B. Newton, Z. Fan, H. Yu, P. C. Ray, R. Gao, *Chem. Commun.*, **2011**, 47, 10311. (e) S. Thyagarajan, T. Leiding, S. P. Arskold, A. V. Cheprakov, S. A. Vinogradov, *Inorg. Chem.*, **2010**, 49, 9909. (f) J. Bhuyan, S. Sarkar, *Chem. An Asian J.*, **2012**, 7, 2690. (g) W. L. Sitienei, L. M. Wangatia, T. Zeng, B. Sun, M. Zhu, *Adv. Mater. Res.*, **2013**, 668, 696. (h) S. E. Rodrigues, A. E. H. Machado, M. Berardi, A. S. Ito, L. M. Almeida, M. J. Santana, L. M. Liao, N. N. M. Barbosa, P. J. Goncalves, *J. Mol. Struct.*, **2015**, 1084, 284. (i) F. Dini, G. Magna, E. Martinelli, G. Pomario, C. Di Natale, R. Paolesse, I. Lundstrom, *Anal. Bioanal. Chem.*, **2015**, 407, 3975.
4. (a) D. Gust, A. Thomas, A. L. Moore, H. K. Kang, J. M. DeGraziano, P. A. Liddell, G. R. Seely, *J. Phys. Chem.*, **1993**, 97, 13637. (b) M. Inamo, A. Tomita, Y. Inagaki, N. Asano, K. Suenaga, M. Tabata, S. Funahashi, *Inorg. Chim. Acta*, **1997**, 256, 77. (c) J. J. A. van Kampen, T. M. Luiders, P. J. A. Ruttink, P. C. Burgers, *J. Mass Spect.*, **2009**, 44, 1556 (d) Z. Valicsek, O. Horvath, *Macrochem. J.*, **2013**, 107, 47 and others.
5. (a) Q. Yan, J. Yuan, Y. Kang, Z. Cai, L. Zhou, Y. Yin, *Chem. Commun.*, **2010**, 46, 2781. (b) Y. Iijima, H. Sakaue, *Sensors and Actuators, A: Phys.*, **2012**, 184, 128. (c) F. Hammerer, G. Garcia, P. Charles, A. Sourdon, S. Achelle, M.-P. Teulade-Fichou, P. Maillard, *Chem. Commun.*, **2014**, 50, 9529 and others.
6. (a) S. Yang, Y. Wo, M. E. Meyerhoff, *Anal. Chim. Acta*, **2014**, 843, 89. (b) Y. F. Huan, Q. Fei, H. Y. Shan, B. J. Wang, H. Xu, G. D. Feng, *Analyst*, **2015**, 140, 1655. (c) S. Rangasamy, H. Ju, S. Um, D.-C. Oh, J. M. Song, *J. Med. Chem.*, **2015**, 58, 6864.
7. (a) H. Imahori, H. Higuchi, Y. Matsuda, A. Itagaki, Y. Sakai, J. Ojima, Y. Sakata, *Bull. Chem. Soc. Jpn.*, **1994**, 67, 2500. (b) H. Higuchi, K. Shimizu, J. Ojima, K. Sugiura, Y. Sakata, *Tetrahedron Lett.*, **1995**, 36, 5359. (c) H. Higuchi, M. Takeuchi, J. Ojima, *Chem. Lett.* **1996**, 593. (d) H. Higuchi, K. Shimizu, M. Takeuchi, J. Ojima, K. Sugiura, Y. Sakata, *Bull. Chem. Soc. Jpn.*, **1997**, 70, 1923. (e) H. Higuchi, M. Takeuchi, Y. Hasegawa, J. Ojima, *Nonlinear Optics*, **1999**, 22, 333. (f) H. Higuchi, M. Shinbo, M. Usuki, M. Takeuchi, Y. Hasegawa, K. Tani, J. Ojima, *Bull. Chem. Soc. Jpn.*, **1999**, 72, 1887. (g) H. Higuchi, T. Ishikura, K. Miyabayashi, M. Miyake, K. Yamamoto, *Tetrahedron Lett.*, **1999**, 40, 9091. (h) H. Higuchi, M. Shinbo, M. Usuki, M. Takeuchi, K. Tani, K. Yamamoto, *Bull. Chem. Soc. Jpn.*, **2000**, 73, 1259. (i) H. Higuchi, T. Ishikura, K. Mori, Y. Takayama, K. Yamamoto, K. Tani, K. Miyabayashi, M. Miyake, *Bull. Chem. Soc. Jpn.*, **2001**, 74, 889. (j) H. Higuchi, T. Maeda, K. Miyabayashi, M. Miyake, K. Yamamoto, *Tetrahedron Lett.*, **2002**, 42, 3097. (k) N. Hayashi, H. Nakashima, Y. Takayama, H. Higuchi, *Tetrahedron Lett.*, **2003**, 44, 5423. (l) N. Hayashi, A. Matsuda, E. Chikamatsu, K. Mori, H. Higuchi, *Tetrahedron Lett.*, **2003**, 44, 7155. (m) N. Hayashi, A. Naoe, K. Miyabayashi, M. Yamada, M. Miyake, H. Higuchi, *Tetrahedron Lett.*, **2004**, 45, 8215. (n) N. Hayashi, A. Naoe, K. Miyabayashi, M. Miyake, H. Higuchi, *Tetrahedron Lett.*, **2005**, 46, 6961. (o) N. Hayashi, M. Sato, K. Miyabayashi, M. Miyake, H. Higuchi, *Sci. Tec. Adv. Mat.*, **2006**, 7, 237. (p) N. Hayashi, T. Nishihara, T. Matsukihira, H. Nakashima, K. Miyabayashi, M. Miyake, H. Higuchi, *Bull. Chem. Soc. Jpn.*, **2007**, 80, 371. (q) V. Borovkov, T. Yamamoto, H. Higuchi, Y. Inoue, *Org. Lett.*, **2008**, 10, 1283.
8. (a) N. Hayashi, T. Matsukihira, K. Miyabayashi, M. Miyake, H. Higuchi, *Tetrahedron Lett.*, **2006**, 47, 5585. (b) H. Higuchi, N. Hayashi, T. Matsukihira, T. Kawakami, T. Takizawa, J. Saito, K. Miyabayashi, M. Miyake, *Heterocycles*, **2008**, 76, 353.
9. (a) N. Hayashi, H. Nishi, K. Morizumi, I. Kobayashi, H. Sakai, R. Akaike, K. Tani, H. Higuchi, *Chemistry Book: Recent Research Developments in Organic Chemistry*, Chapter 16, ed. Pandalai, S. G., *Transworld Research Network (Kerala)*, 2004, 8, 401-424. (b) N. Hayashi A. Matsuda, E. Chikamatsu, M. Murayama, K. Mori, K. Tani, K. Miyabayashi, M. Miyake, H. Higuchi, *Tetrahedron*, **2004**, 60, 6363.
10. (a) In "Determination of Organic Structures by Physical Methods", ed. E. D. Braude and F. C. Nachod, Academic Press (New York), 1955. (b) W. P. Jencks and J. Regenstein, In *Handbook of Biochemistry and Molecular Biology*, ed. R. L. Lundblad and F. M. MacDonald, CRC Press (New York), 4th Ed., Chapter 67; Ionization Constants of Acids and Bases, pp 595-635.
11. H. Kempe, J. Yoshino, N. Hayashi, and H. Higuchi, *Tetrahedron*, **2015**, 71, 1322.
12. To our best knowledge, the $pK_{a(1)}$ and $pK_{a(2)}$ values of conjugated acid of BisDMAB are unknown yet. The pK_a value (4.58) of conjugated acid aniline- H^+ with aniline in water at 25 C is known to be slightly smaller, *i.e.*, a little higher acidity, as compared with that of 5.15 between DMAB and DMAB- H^+ . Thus, based on this fact, the $pK_{a(1)}$ and $pK_{a(2)}$ values of BisDMAB could be slightly larger than those ($pK_{a(1)}$ 2.65 and $pK_{a(2)}$ 4.88) of corresponding 1,3-phenylenediamine.¹⁰
13. (a) J. W. Buchler, In *Porphyrin and Metalloporphyrins*, K. M. Smith, ed. Elsevier: Amsterdam, The Netherlands, 1975, pp 157-231. (b) J. W. Buchler, In *The Porphyrins*, D. Dolphin, ed. Academic: New York, NY, 1978, pp 389-483.
14. M. Gouterman, In *The Porphyrins*, D. Dolphin, ed. Academic: New York, NY, 1978, pp 1-165.
15. (a) 7g. (b) N. Hayashi, K. Tachibana, T. Tsuchiya, K. Miyabayashi, M. Miyake, T. Takizawa, J. Saito, H. Higuchi, *Sci. Tec. Adv. Mat.*, **2007**, 8, 296. (c) H. Kempe, N. Kuroda, J. Yoshino, N. Hayashi, H. Higuchi, *Tetrahedron Lett.*, **2014**, 55, 5164.
16. D. P. Arnold, A. W. Johnson, M. Mahendran, *J. Chem. Soc., Perkin Trans. 1*, **1978**, 366.
17. Prepared from *p*-bromiodobenzene: (a) S. Thorand, N. Krause, *J. Org. Chem.*, **1998**, 63, 8551. (b) B. Zhou, H. Chen, C. Wang, *J. Am. Chem. Soc.*, **2013**, 135, 1246.
18. Prepared from 9,10-dibromoanthracene: S. Destri, W. Porzio, L. Khotina, C. Botta, R. Consonni, *Macromol. Chem. Phys.*, **2001**, 202, 2572.
19. G. Eglinton, A. R. Galbraith, *Chem. Ind.*, **1956**, 737.
20. K. Sonogashira, Y. Tohda, N. Hagihara, *Tetrahedron Lett.* **1975**, 4467.
21. **20**: Purchased as HCl salt from Sigma-Aldrich Fine Chemicals Co., Ltd., Product No. 530921-1 and used for the reaction as it is. **21**: Purchased from Sigma-Aldrich Fine Chemicals Co., Ltd., Product No. 592609-1. **22**: H.

- K. Kim, S. K. Kim, J. H. Park, S. W. Yoon, M. H. Lee, Y. Do, *Chem. Asian J.*, **2008**, 3, 1912.
22. (a) L. D. Ciana and A. Haim, *J. Heterocycl. Chem.*, 1984, **21**, 607. (b) E. Merkul, D. Urselmann, T. J. J. Muller, *Eur. J. Org. Chem.*, **2011**, 238.
23. J. G. Rodriguez, J. L. Tejedor, A. Rumero, L. Canoira, *Tetrahedron*, **2006**, 62, 3075.
24. For Winmoster program: (a) N. Senda, *Idemitsu Technical Report*, **2006**, 49, 106. For PM7 program (MOPAC2012): (b) J. D. C. Maia, G. A. U. Carvalho, C. P. Manguiera, Jr., S. R. Santana, L. A. F. Cabral, G. B. Rocha, *J. Chem. Theory Comput.*, **2012**, 8, 3072. (c) J. J. P. Stewart, *J. Mol. Model.*, **2013**, 19, 1.
25. (a) H. Fukumoto, R. Hoffmann, *J. Phys. Chem.*, **1974**, 78, 1167. (b) H. Fukumoto, S. Kato, S. Yamabe, K. Fukui, *J. Chem. Phys.*, **1974**, 60, 572.
26. At present, it is extremely hard to reach the steady solutions with the full structure of **1-10** by the usual calculation methods, generally due to not only their large molecular formula but also poor parameters for metalloporphyrin ring.
27. J. Yoshino, M. Tsujiguchi, N. Hayashi, H. Higuchi, *Chem. Lett.*, **2011**, 40, 944.
28. (a) J. Rosenthal, E. R. Young, D. G. Nocera, *Inorg. Chem.*, **2007**, 46, 8668. (b) T. D. Lash, A. L. Von Ruden, *J. Org. Chem.*, **2008**, 73, 9417. (c) M. Krouit, R. Granet, P. Krausz, *Eur. Polym. J.*, **2009**, 45, 125. (d) P. J. Chmielewski, J. Maciolek, L. Sztarenberg, *Eur. J. Org. Chem.*, **2009**, 3930. (e) D. K. Singh, M. Nath, *Beil. J. Org. Chem.*, **2015**, 11, 1434. (f) G. Battogtokh, Y. T. Ko, *J. Mater. Chem. B*, **2015**, 3, 9349.
29. (a) G. W. Wheland, *J. Am. Chem. Soc.*, **1941**, 63, 2025. (b) J. L. Franklin, *J. Am. Chem. Soc.*, **1950**, 72, 4278. (c) G. W. Wheland, "Resonance in Organic Chemistry", John Wiley & Sons: New York, NY, 1955, 830 pp. (d) Resonance energies of 36 kcal/mol for benzene, 28 kcal/mol for thiophene, and 83.5 kcal/mol for anthracene are generally employed for discussion. According to these empirical and/or theoretical estimates, the central Phen moiety in anthracene is kinetically ready for taking part in π -electronic conjugation for extension with an external π -electronic system just by losing 11.5 kcal/mol or so at least. Then, the extension efficiency in π -electronic conjugation over the molecule should be achieved thermodynamically, depending on the energy gain by reformation of the electronic structure between the components OEP, SPC, and LB, through the diacetylene linkage.

Graphical Abstract

<Title> Cooperative Effect of Spacer and Lewis Base on Highly Reversible Spectral Changes of The Octaethylporphyrin Chromatic System in Sensitivity, Stability, and Visibility to Trifluoroacetic Acid

<Authors' names> H. Kempe, J. Yamamoto, M. Ishida, N. Takahashi, J. Yoshino, N. Hayashi, H. Higuchi*

<Summary> The [octaethylporphyrin]-[spacer]-[Lewis base] chromatic system (OEP-SPC-LB) was conclusively studied, in which a trigger-like interaction of the terminal LB with trifluoroacetic acid (TFA) dramatically affects the inherent electronic properties of OEP. The structural elements for molecular design were proposed in order to improve their reversible spectral changes between neutral and acidic media in terms of sensitivity, stability, and visibility to TFA.

<Diagram>

